DOI: 10.1002/chem.200701027

VIP

Ambiphilic Diphosphine–Borane Ligands: Metal→Borane Interactions within Isoelectronic Complexes of Rhodium, Platinum and Palladium

Sébastien Bontemps,[a] Marie Sircoglou,[a] Ghenwa Bouhadir,[a] Horst Puschmann,[b] Judith A. K. Howard,[b] Philip W. Dyer,*[b] Karinne Miqueu,*[c] and Didier Bourissou*[a]

Abstract: Coordination of an ambiphilic diphosphine–borane (DPB) ligand to the RhCl(CO) fragment affords two isomeric complexes. According to X-ray diffraction analysis, each complex adopts a square-pyramidal geometry with *trans* coordination of the two phosphine buttresses and axial RhB contacts, but the two differ in the relative orientations around the rhodium and boron centres. DFT calculations on the actual complexes provide insight into the influence of the π-accepting CO co-ligand, compared with previously reported complexes [Rh(μ-Cl)(dpb)]$_2$ and [RhCl(dmap)(dpb)]. In addition, comparison of the $\tilde{\nu}$(CO) frequency of [RhCl(CO)(dpb)] with that of the related borane-free complex [RhCl(CO)(*i*Pr$_2$PPh)$_2$] substantiates the significant electron-withdrawing effect that the σ-accepting borane moiety exerts on the metal. Valence isoelectronic [PtCl$_2$(dpb)] and [PdCl$_2$(dpb)] complexes have also been prepared and characterized spectroscopically and structurally. The pronounced influence of the transition metal on the magnitude of the M→B interaction is highlighted by geometric considerations and NBO analyses.

Keywords: ambiphilic ligands · boranes · density functional calculations · transition metals · X-ray diffraction

Introduction

The ability of Group 13 Lewis acids ER$_3$ (E = Al, B, etc.) to act as σ-acceptor ligands for transition metals (TM)[1] was recognized as early as 1979 by Burlitch and Hughes who reported structural evidence for a Fe→Al interaction in complex A[2] (Figure 1). Examples of such unusual M→ER$_3$ interactions remain, however, extremely rare. Only one other alane complex B,[3] featuring two bridging hydrides, has been authenticated to date, while the structural characterization[4,5] of the first borane complex C (with ML$_n$ = [Ru(CO)(PPh$_3$)][6] dates from only 1999. However, following the pioneering work of Hill et al., the activation of B–H bonds of poly(azolyl)borate ligands has been used as a general pathway to prepare a variety of metallaboratranes C (with M = Fe, Ru, Os, Co, Rh, Ir, Pd, Pt).[7] The related complex D featuring only two methimazolyl buttresses was also found to exhibit an Ir→B interaction.[7k] Notably, the contribution of

[a] Dr. S. Bontemps, M. Sircoglou, Dr. G. Bouhadir, Dr. D. Bourissou
Laboratoire Hétérochimie Fondamentale
et Appliquée du CNRS (UMR 5069)
Equipe Ligands Bifonctionnels et Polymères
Biodégradables
Université Paul Sabatier
118 route de Narbonne, 31062 Toulouse Cedex 09 (France)
Fax: (+33) 5-61-55-82-04
E-mail: dbouriss@chimie.ups-tlse.fr

[b] Dr. H. Puschmann, Prof. Dr. J. A. K. Howard, Dr. P. W. Dyer
Department of Chemistry
Durham University
South Road, Durham, DH1 3LE (UK)
E-mail: p.w.dyer@durham.ac.uk

[c] Dr. K. Miqueu
Equipe de Chimie-Physique (UMR 5254-IPREM)
Université de Pau et des Pays de l'Adour
Avenue de l'Université, BP 1155
64013 Pau Cedex (France)
E-mail: karinne.miqueu@univ-pau.fr

Supporting information for this article is available on the WWW under http://www.chemistry.org or from the author.

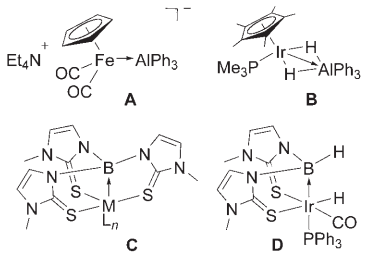

Figure 1. Structurally authenticated complexes A–D featuring M→AlR$_3$ and M→BR$_3$ interactions.

M→B interactions[8–10] has also been pointed out in the bonding description of tantalocene–borataalkene η^2-complexes[11a] and of boryl-bridged complexes.[11b–d] In this context, we have recently initiated a research programme aimed at exploring the use of so-called ambiphilic ligands combining donor and acceptor coordination sites.[12–15] Here, the rhodium complexes **2** and **3**,[12a] deriving from the diphosphine-borane (DPB) **1**, provided the first evidence for M→B interactions in the absence of a σ-donor in the position *trans* to the Lewis acid. Moreover, the gold complexes **5**,[12b] deriving from related monophosphine-boranes **4**, exemplify the possibility for M→B interactions to occur in 14e complexes, even when supported by only a single donor buttress (Scheme 1). In addition, the Lewis acidic component of

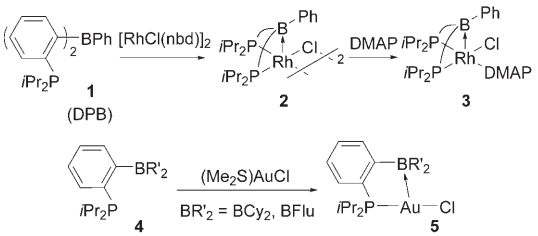

Scheme 1. Rhodium complexes **2** and **3** deriving from the diphosphine–borane (DPB) ligand **1** and gold complexes **5** deriving from the related monophosphine ligands **4**.

ambiphilic ligands has been shown to eventually interact with other basic centres located within the coordination sphere (such as a chloride ligand[12b,d,15b] or the oxygen atom of a coordinated dibenzylideneacetone[15a]), a situation that opens interesting perspectives in organometallic catalysis.[16,17] The coordination of preformed ambiphilic ligands affords access to a broad variety of TM complexes featuring coordinated Lewis acids, thereby offering a unique opportunity to gain a better understanding of such unusual M→ER_3 interactions. In this context, we report here the synthesis and complete characterization of the [RhCl(CO)(dpb)] complex,[18] providing spectroscopic and structural evidence for i) *trans* coordination of the DPB ligand, ii) the existence of two isomeric structures differing only in their relative orientations around the rhodium and boron centres, iii) the noticeable influence of the CO co-ligand on the Rh→B interaction, and iv) the quantification of the electron-withdrawing effect of the σ-accepting borane moiety through analysis of the $\tilde{\nu}$(CO) frequency. The related [$PtCl_2$(dpb)] and [$PdCl_2$(dpb)] complexes have also been investigated, both experimentally and computationally, the results highlighting the strong influence of the metal (Rh/Pt/Pd) on the magnitude of M→B interactions, even within this isoelectronic series.

Results and Discussion

Synthesis and structural characterization of [RhCl(CO)(dpb)] complex 6: Since Tolman's pioneering contribution,[19] IR analysis of carbonyl complexes has become one of the most widely used methods of probing the electronic properties of σ-donor ligands. For example, this approach was used to demonstrate that *N*-heterocyclic carbenes are significantly stronger donor ligands than phosphines,[20] and was even highlighting the subtle skeleton and substituent effects among various carbene ligands.[21] Thus, in order to estimate the electron-withdrawing effect of the borane moiety of the DPB ligand, we envisaged the preparation of a rhodium carbonyl complex related to **2** and **3** such that its carbonyl stretching frequency could be compared with that of the corresponding complex [RhCl(CO)($iPr_2PPh)_2$] that has no σ-accepting co-ligand. The desired complex [RhCl(CO)(dpb)] **6** was obtained by reaction of **1** with half an equivalent of the rhodium(I) precursor [Rh(μ-Cl)$(CO)_2]_2$ in dichloromethane at room temperature (Scheme 2). Surprising-

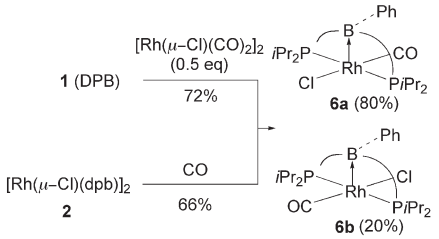

Scheme 2. Synthesis of the complex [RhCl(CO)(dpb)] **6**.

ly, the ^{31}P NMR spectrum of the crude reaction mixture displays two doublets at δ 46.8 and 50.3 ppm with identical Rh–P coupling constants [^1J(Rh,P) = 102 Hz], but of markedly different relative intensity (ca. 8:2). These data suggest that [RhCl(CO)(dpb)] **6** exists in two similar forms and that the DPB ligand is symmetrically coordinated to the rhodium centre (with a *trans* arrangement of the two phosphorus atoms). Variable temperature ^{31}P NMR studies demonstrate that the 8:2 ratio between both forms of the complex remains unchanged upon heating to 70 °C, suggesting that interconversion does not occur readily. Attempted separations of the two components prepared as above by fractional recrystallization were unsuccessful. Consequently, attempts were made to prepare a single form of [RhCl(CO)(dpb)] **6** by cleavage of the chloride bridge of **2** with carbon monoxide, but once again this led to an identical 8:2 mixture of both complexes. To gain more insight into the structure of complex **6**, an X-ray diffraction analysis was carried out on the yellow crystals obtained at room temperature from a dichloromethane/diethyl ether solution of the mixture (Figure 2, Table 1). This revealed that the rhodium centre is located in a square-pyramidal environment with the boron atom occupying the pseudo-axial position (PRhB bond angles of 87 and 84°). The geometry of **6** is entirely consis-

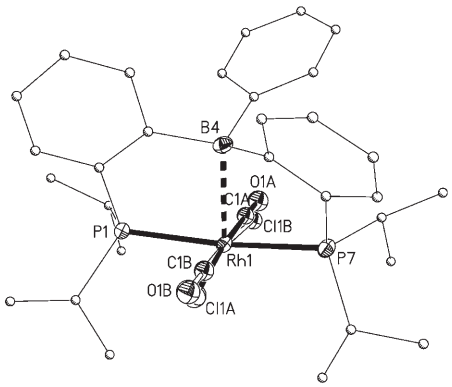

Figure 2. Molecular structure of the complexes [RhCl(CO)(dpb)] **6a/6b** with hydrogen atoms omitted.

Table 1. Geometric data (bond lengths and angles in Å and °, respectively) determined experimentally for complexes **2**, **3** and **6a/6b** and computed at the B3PW91/SDD(Rh),6-31G**(other atoms) level of theory for actual complexes **3*** and **6a–c***.

	2	**3**	**3***	**6a/6b**	**6a***	**6b***	**6c***
Rh−B	2.306(3)	2.295(5)	2.292	2.374(3)	2.397	2.357	2.366
Rh−P	2.251(2)	2.286(2)	2.337	2.332(1)	2.350	2.357	2.450
	2.271(2)	2.256(2)	2.278	2.327(1)	2.349	2.362	2.270
PRhP	98.5(1)	97.6(1)	101.7	168.9(1)	167.5	169.0	104.1
PRhB	81.2(1)	80.1(2)	81.4	87.0(2)	84.0	80.1	82.3
	80.4(1)	83.6(2)	84.1	84.0 (1)	86.6	83.6	83.1
PCC	112.2(2)	112.5(3)	113.7	116.7(2)	116.7	116.3	114.1
	112.8(2)	114.1(3)	113.0	116.2(2)	116.3	117.4	115.5
CCB	121.8(3)	119.3(4)	123.4	122.5(2)	127.7	121.6	125.8
	120.8(3)	122.3(4)	122.6	127.7(2)	124.1	121.2	124.5
ΣB_α	338.8(9)	338.8(9)	339.2	342.6(2)	343.6	343.8	343.8

tent with the spectroscopic data, and is in marked contrast with that observed in complexes **2** and **3**, where a *cis*-coordination of DPB is observed.[22] The two phosphine moieties span *trans* sites in **6** with a quasi-linear PRhP arrangement (bite angle 169°). Clearly, despite the apparent rigidity of the diphenylborane spacer, DPB can readily adopt both *cis* (**2** and **3**) and *trans* (**6**) coordination modes.[23,24] Notably, the CO and Cl ligands around rhodium are disordered, with the CO group principally occupying the position *syn* to the phenyl ring at boron (compound **6a**).[25] This disorder results in a ca. 85:15 ratio of diastereomeric compounds **6a** and **6b** (featuring a *syn* arrangement of the chlorine atom and phenyl ring at boron), a situation that nicely parallels that observed in solution by ^{31}P NMR spectroscopy. The Rh–B distance in **6a/6b** (2.374 Å) and the pyramidalization of the boron environment (sum of CBC bond angles $\Sigma B_\alpha = 342.6°$) are clearly indicative of a Rh→B interaction, which is apparently strong enough to prevent inversion of configuration at boron, and therefore interconversion between **6a** and **6b**. Comparison of these geometric features with those of related complexes **2** and **3** (Table 1) suggests a slightly weaker Rh→B interaction in [RhCl(CO)(dpb)], a trend that is also apparent in solution from the displacement to higher frequency of the ^{11}B NMR signal ($\delta = 26.7$ ppm for **6a/6b** vs 20.0 and 19.4 ppm for **2** and **3**, respectively). At a first glance, this situation may simply reflect the influence of the π-accepting CO co-ligand that decreases the electron density at rhodium. However, a more reliable comparison between complexes **6a/6b** and **2**, **3** requires the precise influence of the geometric constraints associated with *trans* vs *cis* coordination of the DPB ligand to be determined.

DFT calculations on [RhCl(CO)(dpb)] complex 6: To gain more insight into the isomeric structures of [RhCl(CO)(dpb)] and the geometric/electronic influence of the CO co-ligand, DFT calculations were performed on the actual mononuclear complexes **3** and **6**. Here, the B3PW91/SDD(Rh),6-31G**(other atoms) level of theory was found to reproduce particularly well the key features of the [RhCl(dmap)(dpb)] complex **3**, with a maximum deviation of only 0.05 Å for the Rh–P distances, and virtually no deviations for the Rh–B distance and boron pyramidalization relative to that determined by X-ray crystallography (Table 1). For the related complex [RhCl(CO)(dpb)] **6**, three minima were located on the potential energy surface (Figure 3). In agreement with experimental observations, the most stable form is the *trans* isomer **6a*** featuring a *syn* arrangement of the CO co-ligand and phenyl group at boron. The other *trans* isomer **6b*** and the *cis* isomer **6c*** are located 2.5 and 11.8 kcal mol^{-1} higher in energy, respectively. The geometric data computed for **6a*** and **6b*** are very similar (with a maximum deviation of only 0.04 Å for the Rh–B distance), and agree well with those determined experimentally for **6a/6b**. For the related *cis* isomer, the two Rh-P distances differ significantly (by about 0.2 Å), as ex-

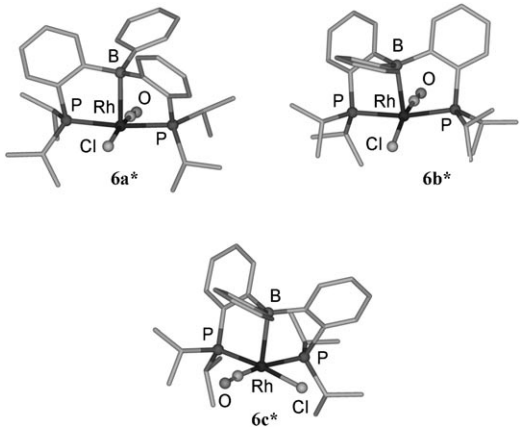

Figure 3. Optimized structures of the three isomeric structures **6a–c*** of the actual complex [RhCl(CO)(dpb)], with hydrogen atoms omitted.

pected due to the different *trans* influences of CO and Cl, but the Rh–B distance (2.366 Å) and boron pyramidalization ($\Sigma B_\alpha = 343.8°$) remain practically unchanged.[26] These results indicate that the *cis*/*trans* coordination of the DPB ligand induces only weak geometric constraints and corroborate the notion that the slight elongation of the Rh–B distance on going from **3** to **6** is a result of the presence of the π-accepting carbonyl co-ligand. In addition to these geometric considerations, the magnitude of the Rh–B interaction in the complex [RhCl(CO)(dpb)] **6** was assessed via second-order perturbative natural bond orbital (NBO) analyses. For each of the structures **6a***, **6b*** and **6c***, a donor–acceptor interaction was found between the rhodium and boron centres (Figure 4). The corresponding natural localized molecular orbitals (NLMO) are very similar with a major contribution from the rhodium d_{z^2} orbital (83–84%) and "delocalization tails" (11–13%) from a slightly hybridized vacant orbital at boron (11.5–12.2% s character) (Table 2). The NBO delocalization energies ΔE associated with the Rh→B interaction are about 46 kcal mol^{-1} for both *trans* isomers **6a*** and **6b***, and 68 kcal mol^{-1} for the related *cis* complex **6c*** (a difference mainly attributable to the ΔE_{ij} term, which corresponds to the energy separation between the donor and acceptor orbitals). All these calculated ΔE values are significantly lower than those determined for the related [RhCl(dmap)(dpb)] complex **3*** (86 kcal mol^{-1}, at the same level of theory), confirming that the π-accepting CO co-ligand weakens the Rh→B interaction.

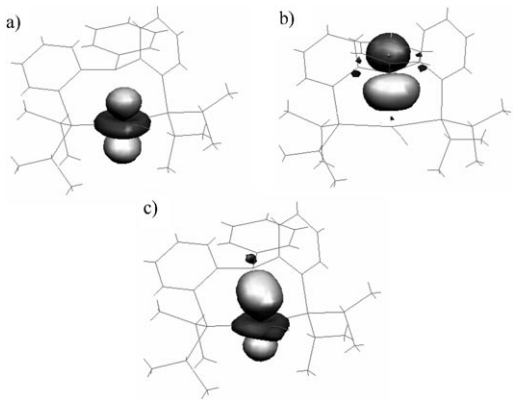

Figure 4. Molekel plots (cutoff: 0.05) for the a) donor NBO, b) acceptor NBO and c) corresponding NLMO associated with the Rh→B interaction in the complex [RhCl(CO)(dpb)] **6a***.

Spectroscopic studies of complexes [RhCl(CO)(dpb)] 6: The electron-withdrawing effect of the borane moiety in complex **6** has also been assessed through measurement of its carbonyl stretching frequency (IR). The mixture **6a**/**6b** exhibits a single $\tilde{\nu}$(CO) band at 2001.8 cm^{-1} in chloroform.[27] In comparison, the $\tilde{\nu}$(CO) band appears at 1966.7 cm^{-1} for the related complex *trans*-[RhCl(CO)-(*i*Pr$_2$PPh)$_2$] that has no σ-accepting co-ligand. The shift of 35 cm^{-1} to higher carbonyl stretching frequency demonstrates that the Rh→B interaction withdraws a significant amount of electron density from rhodium. This observation is consistent with the σ-accepting borane moiety of DPB somewhat compensating for the presence of the two σ-donating dialkylphosphine moieties, such that the combined electronic characteristics of the DPB ligand resemble, to some extent, those of π-accepting diphosphonites or diphosphites.[28] These results provide the first reliable estimation of the electron-withdrawing effect of borane coordination.[29,30]

Synthesis and characterization of [PtCl$_2$(dpb)] 7 and [PdCl$_2$-(dpb)] 8: As observed with the rhodium complexes **2**, **3** and **6**, coordination of the DPB ligand involves a Rh→B interaction, whose magnitude is somewhat affected by the nature of the co-ligands. To further demonstrate the propensity of DPB to act as an ambiphilic tridentate PBP ligand, related platinum and palladium complexes were then investigated. The $PtCl_2$ and $PdCl_2$ fragments were chosen in order to evaluate the influence of the metal within a valence isoelectronic d^8 ML_4 series. The DPB ligand **1** was thus treated with one equivalent of the platinum(II) and palladium(II) precursors [MCl$_2$(cod)] (cod = 1,5-cyclooctadiene) in dichloromethane at low temperature (Scheme 3). Subsequently, the target complexes [MCl$_2$(dpb)] (M = Pt, **7**; M = Pd, **8**) were isolated as white and yellow powders, respectively. The low isolated yield of the palladium complex (26%) results from the formation of a substantial amount of an, as yet, unidentified complex exhibiting two doublets at δ 34 and −43 ppm with a J(P,P) coupling constant of 286 Hz in its ^{31}P NMR spectrum. Both complexes **7** and **8** have been fully characterized by multinuclear NMR spectroscopy, with their ^{1}H NMR spectra confirming the displacement of the labile cyclooctadiene ligand by **1**. In their ^{31}P NMR spectra, the two phosphorus atoms of coordinated DPB were found to be magnetically inequivalent (**7**: δ = 39.7/38.8 ppm and **8**: 61.1/

Table 2. NBO analysis of the M→B interaction for actual complexes **3***, **6a–c***, **7*** and **8*** at the B3PW91/SDD(M),6-31G**(other atoms) level of theory.

	ΔE[a]	% M[b]	% B[b]	occ. M[c]	occ. B[c]	ΔE_{ij}[d]	F_{ij}[e]	q(B)[f]	Bond order[g]
3*	85.6	80.4	16.8	1.652	0.524	0.17	0.11	0.55	0.44
6a*	46.4	84.6	10.8	1.726	0.444	0.20	0.09	0.62	0.33
6b*	46.8	83.4	11.3	1.704	0.469	0.21	0.09	0.59	0.32
6c*	67.7	84.6	13	1.729	0.463	0.18	0.10	0.60	0.34
7*	49.6	87.5	10.3	1.785	0.430	0.26	0.11	0.62	0.28
8*	13.6	93.1	5.5	1.879	0.346	0.27	0.05	0.72	0.18

[a] NBO stabilizing energy associated with the M→B interaction, in kcal mol^{-1}. [b] Percentage of the donor and acceptor NBO in the corresponding NLMO. [c] Occupancy of the donor and acceptor NBO orbitals. [d] Energy difference between the donor and acceptor NBO orbitals, in a. u. [e] Off-diagonal NBO Fock matrix element. [f] NPA atomic charge of boron. [g] Atom–atom net linear bond order based on the NLMO/NPA.

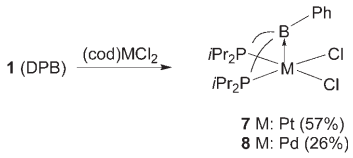

Scheme 3. Synthesis of the complexes $[PtCl_2(dpb)]$ **7** and $[PdCl_2(dpb)]$ **8**.

56.0 ppm). A similar situation was observed in the related rhodium complex **2**,[12a] and is something most likely attributable to different conformations of the two phenyl linkers of the coordinated DPB ligand. The low ^2J(P,P) coupling constants observed for **7** and **8** (9.0 and 6.5 Hz, respectively) are diagnostic of *cis* coordination.[31] This *cis* coordination in complex **7** is further supported by the observed ^1J(Pt,P) coupling constants (3323 and 3081 Hz) that are very similar to those reported for the *cis*-$[PtCl_2(Ar_2PCH_2PAr_2)]$ complex [Ar = *o*-*i*PrPh, ^1J(Pt,P) = 3045 and 3337 Hz].[32] In addition, the ^{195}Pt NMR spectrum of **7** showed a resonance at $\delta = -3957$ ppm, in the same region as that reported by Hill for a metallaboratrane featuring a Pt→B interaction ($\delta = -3899$ ppm).[7b] In solution, the Pt and Pd complexes exhibit broad resonances in their ^{11}B NMR spectra at δ 43 and 47 ppm, respectively. Although these values appear comparable with that of the free ligand DPB (43 ppm), this is somewhat misleading since DPB exists in solution as a mixture of "closed" and "open" forms (i.e., with or without intramolecular P→B interaction).[12c] More significantly, the ^{11}B NMR chemical shifts of **7** and **8** fall half-way between those observed for the frozen "open" form of DPB (solid-state, 71 ppm) and the rhodium complexes (**2**: 20.0 ppm, **3**: 19.4 ppm, **6a/6b**: 26.7 ppm). Together these observations are consistent with weak metal→boron interactions for both the platinum and palladium complexes **7** and **8**. To gain greater insight into the precise structures of **7** and **8**, single crystals suitable for X-ray diffraction analyses were grown from a saturated THF solution of **7** at −40 °C and by slow diffusion of pentane into a dichloromethane solution of **8**. Molecular views are shown in Figure 5, with selected bond lengths and angles given in Table 3. The overall geometry of the two complexes is similar and analogous to that of the *cis*-rhodium complexes **2** and **3**. The Pt and Pd atoms adopt slightly distorted square-pyramidal geometries, with the phosphorus and chlorine atoms forming the coordination plane ($\Sigma Pt_\alpha = 360.3°$, $\Sigma Pd_\alpha = 360.1°$) and the boron atom occupying the pseudo-axial position. As suggested by the spectroscopic data, the two phosphorus atoms of the DPB ligand adopt a *cis* arrangement with bite angles (PPtP = 99.4° and PPdP = 99.6°) very similar to those of the related rhodium complexes (PRhP = 98.5° in **2** and 97.6° in **3**). In both complexes **7** and **8**, the DPB ligand is folded so that the boron is included in the first coordination sphere of the metal, the boron–metal axis being almost perpendicular to the square coordination plane (PPtB = 80.7/82.4° and PPdB = 77.8/80.1°). The presence of an M–B interaction in complex **7** is supported by the short Pt–B distance (2.429 Å compared with 3.72 Å for the sum of van der Waals radii) and the noticeable pyramidalization of the boron environment ($\Sigma B_\alpha = 346.6°$). To the best of our knowledge, complex **7** represents the first structurally characterized platinum–borane complex, although related Pt→B interactions (2.49–2.51 Å) have previously been reported by Norman and Orpen in two boryl-bridged dinuclear complexes.[11b] In contrast, complex **8** exhibits a significantly longer Pd–B distance (2.65 vs 3.63 Å for the sum of van der Waals radii). This value considerably surpasses those found by Parkin et al. in palladaboratranes (2.05–2.07 Å),[7j] and by Braunschweig and coworkers in a boryl-bridged iron-palladium complex (2.06 Å),[11d] but falls in the same range as that observed by

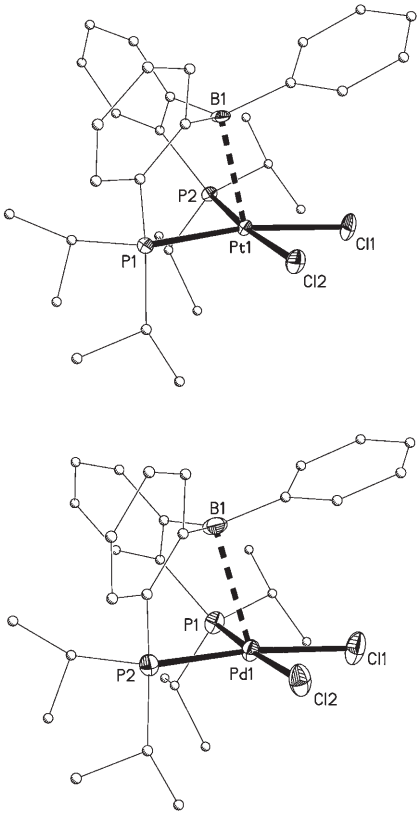

Figure 5. Molecular structures of complexes $[PtCl_2(dpb)]$ **7** (top) and $[PdCl_2(dpb)]$ **8** (bottom) with hydrogen atoms and solvate molecules omitted.

Table 3. Geometric data (bond lengths and angles in Å and °, respectively) determined experimentally for complexes **7** and **8** and computed at the B3PW91/SDD(M),6-31G**(other atoms) level of theory for actual complexes **7*** and **8***.

	7	**7***	**8**	**8***
M–B	2.429(3)	2.488	2.650(3)	2.652
M–P	2.284(1)	2.310	2.288(2)	2.365
	2.304(2)	2.342	2.315(2)	2.323
$B–C_{ipso}$	1.589(5)	1.583	1.558(5)	1.569
PMP	99.4(1)	103.8	99.5(1)	104.1
PMB	80.7(1)	81.0	80.1(1)	76.4
	82.4(1)	78.2	77.8(1)	79.4
ΣB_α	346.6(9)	347.3	354.9(9)	352.6

Braunstein, Herberich et al. in a palladium/rhenium cluster of phenylborole (2.59 Å).[33] Together these comparisons suggest the presence of only a very weak Pd→B interaction in complex **8**, a hypothesis that is confirmed by the noticeable, albeit attenuated, pyramidalization of the boron environment ($\Sigma B_\alpha = 354.9°$). The geometric data collected for the Rh, Pt and Pd complexes of the DPB ligand reveal marked variations in the extent of the M→B interaction, even within such an isoelectronic series. The M–B distance is considerably elongated (from 2.29 Å with Rh, to 2.43 Å with Pt, and 2.65 Å with Pd), suggesting significant weakening of the M→B interaction. This variation is accompanied by a progressive planarization of the boron environment (ΣB_α increasing from 338.8° with Rh, to 346.6° with Pt, and 354.9° with Pd) and by a slight shortening of the BC_{ipso} bond length (from 1.63 Å with Rh, to 1.59 Å with Pt, and 1.56 Å with Pd) suggesting some compensating π-donation from the phenyl substituent to the vacant orbital of boron. As might have been anticipated, the M→B interaction is strengthened with increasing intrinsic basicity of the metal (Pd < Pt < Rh),[34] but the large magnitude of the ensuing geometric variations was somewhat unexpected, the M–B distance being a particularly sensitive probe.

DFT Calculations on complexes [$PtCl_2$(dpb)] 7 and [$PdCl_2$-(dpb)] 8: In order to gain a better insight into the influence of the metal on the M→B interaction than that provided by geometric considerations alone, DFT calculations were carried out on the actual platinum and palladium complexes **7*** and **8***. Again, the key features of both complexes were very well reproduced at the B3PW91/SDD(M),6-31G**(other atoms) level of theory (Table 3), with deviations in the M–B distance of 0.04 Å for the platinum complex and only 0.002 Å for its palladium counterpart. Accordingly, the variations predicted between complexes **3***, **7*** and **8*** for the M–B distance and boron pyramidalization fit perfectly with those revealed by the X-ray data. In addition, second-order perturbative NBO analyses were performed to further evidence the progressive weakening of the M→B interaction from Rh, to Pt, and Pd. By analogy with that observed for rhodium complexes **3*** and **6***, and despite elongated M–B distances, a donor–acceptor M–B interaction was found for both complexes **7*** and **8***. The corresponding NLMO is more and more centred on the metal d_{z^2} orbital (from 80.4% in the Rh complex **3***, to 87.5% in the Pt complex **7***, and 93.1% in the Pd complex **8***), with concomitant attenuation of the contribution of the boron vacant orbital (from 16.8% with Rh, to 10.3% with Pt, and 5.5% with Pd) (Table 2). Accordingly, the NBO delocalization energy associated with the M→B interaction (whose precise value is meaningless) decreases dramatically from 85.6 kcal mol^{-1} with Rh, to 49.6 kcal mol^{-1} with Pt, and 13.6 kcal mol^{-1} with Pd. This variation, which apparently results from both larger ΔE_{ij} terms and smaller F_{ij} terms with the less basic metals, is also apparent from the NPA/NLMO M–B bond orders that drop from 0.44 with Rh, to 0.28 with Pt, and 0.18 with Pd, in agreement with the increase of the M–B distance. In addition, the transfer of some electron density from the metal to the σ-acceptor ligand is indicated by the lower boron atomic charges predicted for complexes **3***, **7*** and **8*** compared with that of the free ligand **1*** (0.85, in its "open" form), the weakening of the M→B interaction from Rh, to Pt, and Pd being accompanied by a noticeable increase of q(B) (from 0.55, to 0.62, and 0.72, respectively).

Conclusion

This combined experimental/theoretical investigation of new rhodium, platinum, and palladium complexes bearing the ambiphilic DPB ligand **1** provides additional information on unusual M→BR_3 interactions. Analysis of the [RhCl(CO)-(dpb)] complex substantiates the noticeable influence that co-ligands may have and allows a spectroscopic estimation of the electron-withdrawing effect of the σ-acceptor borane moiety. Notably, the M→B interactions were found to be significantly weakened in the [$PtCl_2$(dpb)] (**7**) complex and to an even greater extent in [$PdCl_2$(dpb)] (**8**) compared with that for the rhodium complex **6**. The pronounced variations in the M-B distance and the extent of boron pyramidalization within the valence isoelectronic series of Rh, Pt and Pd complexes of DPB contrast markedly with the similarity observed between all metallaboratranes, for which the M–B distances fall within a rather narrow range (2.05–2.21 Å). This demonstrates that the rather strong M→B interactions exhibited by the rhodium complexes **2**, **3** and **6** are supported, but not geometrically imposed, by the skeleton of the DPB ligand. Since a progressive and significant weakening of the M→B interaction has been observed from rhodium, to platinum, and palladium, this suggests that there is a continuum between the two limiting bonding situations described by Hill[35a] and Parkin[35b] for such M→BR_3 interactions, namely: i) retention of the original d^n configuration of the metal and a coordinated neutral BR_3 ligand vs. ii) 2e oxidation of the metal resulting in a d^{n-2} configuration and a dianionic BR_3^{2-} ligand. Further investigations in this area are currently in progress by varying the stereoelectronic properties of the DPB ligand and the metal fragment to which it is coordinated.

Experimental Section

All reactions and manipulations were carried out under an atmosphere of dry argon using standard Schlenk techniques. THF and diethyl ether were dried over sodium/benzophenone, CH_2Cl_2 was dried over P_2O_5 and pentane was dried over CaH_2 and distilled prior to use. ^{1}H, ^{13}C, ^{11}B, ^{31}P, ^{195}Pt NMR and ^{103}Rh spectra were recorded on Bruker Avance 300 or AMX 500 spectrometers. Chemical shifts are expressed with a positive sign, in parts per million, relative to residual ^{1}H and ^{13}C solvent signals and external $BF_3.OEt_2$, 85% H_3PO_4, Na_2PtCl_6, $\Xi = 3.186447$ MHz respectively. Unless otherwise stated, NMR spectra were recorded at 20 °C. Infrared spectra were recorded on a FT-IR Perkin-Elmer 1600 spectrometer. Mass spectra were recorded on Hewlett Packard 5989A. The DPB ligand **1**[12a,c] and the ensuing [Rh(μ-Cl)(dpb)]$_2$ complex[12a] were prepared following literature procedures.

[RhCl(CO)(dpb)] complexes 6a and 6b

Path a: A solution of DPB **1** (160 mg, 0.31 mmol) in CH_2Cl_2 (5 mL) was added at room temperature to a solution of $[Rh(\mu\text{-}Cl)(CO)_2]_2$ (60 mg, 0.15 mmol) in CH_2Cl_2 (5 mL). After subsequent stirring for 30 min, diastereomeric complexes **6a** and **6b** were obtained after removal of volatile components. Yellow crystals (128 mg, 65%) suitable for X-ray crystallography were obtained from a dichloromethane/diethyl ether solution at room temperature. M.p. 228–230°C; IR ($CDCl_3$): $\tilde{\nu}$ = 2001.8 cm^{-1} (CO).

Path b: CO was bubbled slowly through a solution of $[Rh(\mu\text{-}Cl)(dpb)]_2$ (**2**) (50 mg, 0.04 mmol) in CH_2Cl_2 for 5 min affording a mixture of isomeric complexes **6a** and **6b**, which were isolated after the work up described above (34 mg, 66%).

Complex 6a (80%): $^{31}P\{^1H\}$ NMR (202.5 MHz, $CDCl_3$, 23°C): δ = 49.9 ppm (d, ^1J(Rh,P) = 102.4 Hz); ^{11}B NMR (160.5 MHz, $CDCl_3$): δ = 26.7 ppm; ^{103}Rh NMR (15.9 MHz, $CDCl_3$): δ = −8468 ppm; ^1H NMR (500.3 MHz, $CDCl_3$): δ = 7.67 ([pseudo-t]dd, ^3J(P,H) = 3.7, ^3J(H,H) = 7.5, ^4J(H,H) = 1.4 Hz, 2H; H_{arom}), 7.62 (dd, ^3J(H,H) = 7.5, ^4J(H,H) = 1.4 Hz, 2H; H_{arom}), 7.33 (m, 2H; H_{arom}), 7.29 (m, 2H; H_{arom}), 7.12 ([pseudo-t]t, ^3J(H,H) = 8.1, ^4J(H,H) = 1.4 Hz, 1H; H_{arom}), 7.04 ([pseudo-t]d, ^3J(H,H) = 8.1, ^4J(H,H) = 1.4 Hz, 2H; H_{arom}), 6.88 (dd, ^3J(H,H) = 8.1, ^4J(H,H) = 1.4 Hz, 2H; H_{arom}), 3.20 (br, 2H; CH P*i*Pr_2), 2.43 (br, 1H; CH P*i*Pr_2), 1.67 (m, 6H; CH_3 P*i*Pr_2), 1.61 (m, 6H; CH_3 P*i*Pr_2), 1.45 (m, 6H; CH_3 P*i*Pr_2), 1.40 ppm (m, 6H; CH_3 P*i*Pr_2); $^{13}C\{^1H\}$ NMR (125.8 MHz, $CDCl_3$): δ = 189.4 (td, ^1J(Rh,C) = 74.6 Hz, ^2J (P,C) = 12.1 Hz; CO), 164.7 (br; BC_{ipso}), 155.6 (br; BC_{ipso}), 136.3 (s; $2CH_{arom}$), 134.9 (pseudo-t, ^1J(P,C) = 21.7 Hz; PC_{ipso}), 131.3 (pseudo-t, J(P,C) = 9.4 Hz; CH_{arom}), 131.2 (s; arom), 128.8 (s; CH_{arom}), 127.2 (s; CH_{arom}), 126.5 (s; $2CH_{arom}$), 124.6 (pseudo-t, J(P,C) = 7.1 Hz; $2CH_{arom}$), 29.4 (br pseudo-t, ^1J(P,C) = 11.9 Hz; CH P*i*Pr_2), 24.8 (br pseudo-t, ^1J(P,C) = 11.9 Hz; CH P*i*Pr_2), 23.3 (br; CH_3 P*i*Pr_2), 21.4 (br; CH_3 P*i*Pr_2), 19.6 (br; CH_3 P*i*Pr_2), 18.9 ppm (br; CH_3 P*i*Pr_2).

Complex 6b (20%): $^{31}P\{^1H\}$ NMR (202.5 MHz, $CDCl_3$, 23°C): δ = 46.7 ppm (d, ^1J(Rh,P) = 102.4 Hz); ^{11}B NMR (160.5 MHz, $CDCl_3$): δ = 26.7 ppm; ^{103}Rh NMR (15.9 MHz, $CDCl_3$): δ = −8393 ppm; ^1H NMR (500.3 MHz, $CDCl_3$): δ = 7.95 (br d, ^3J(H,H) = 7.7 Hz, 2H; H_{arom}), 7.64 (m, 2H; H_{arom}), 7.41 (br pseudo-t, ^3J(H,H) = 7.7 Hz, 2H; H_{arom}), 7.31 (m, 2H; H_{arom}), 7.08 ([pseudo-t]t, ^3J(H,H) = 7.7 Hz, ^4J(H,H) = 1.4 Hz, 1H; H_{arom}), 6.95 ([pseudo-t]d, ^3J(H,H) = 7.7 Hz, ^4J(H,H) = 1.4 Hz, 2H; H_{arom}), 6.82 (br dd, ^3J(H,H) = 7.7 Hz, ^4J(H,H) = 1.4 Hz, 2H; H_{arom}), 2.98 (br, 2H; CH P*i*Pr_2), 2.82 (br, 1H; CH P*i*Pr_2), 1.68 (m, 6H; CH_3 P*i*Pr_2), 1.54 (m, 6H; CH_3 P*i*Pr_2), 1.55 (m, 6H; CH_3 P*i*Pr_2), 1.33 ppm (m, 6H; CH_3 P*i*Pr_2); $^{13}C\{^1H\}$ NMR (125.8 MHz, $CDCl_3$): δ = 186.4 (td, ^1J(Rh,C) = 69.7 Hz, ^2J(C,P) = 13.3 Hz; CO), 136.9 (s; $2CH_{arom}$), 136.5 (pseudo-t, J(P,C) = 23 Hz; PC_{ipso}), 132.8 (br; CH_{arom}), 130.9 (pseudo-t, J(P,C) = 9 Hz; $2CH_{arom}$), 129.1 (s; CH_{arom}), 127.5 (s, CH_{arom}), 126.0 (s; $2CH_{arom}$), 124.1 (pseudo-t, J(P,C) = 6.9 Hz; CH_{arom}), 27.3 (br pseudo-t, ^1J(P,C) = 10.7 Hz; CH P*i*Pr_2), 24.5 (br pseudo-t, ^1J(P,C) = 12.6 Hz; CH P*i*Pr_2), 22.9 (pseudo-t, ^2J(P,C) = 3.4 Hz; CH_3 P*i*Pr_2), 21.6 (br; CH_3 P*i*Pr_2), 20.3 (br; CH_3 P*i*Pr_2), 19.5 ppm (br; CH_3 P*i*Pr_2). BC_{ipso} are not observed.

[RhCl(CO)(*i*Pr_2PPh)$_2$]: A solution of phenyllithium (2.0 M) in dibutyl ether (0.58 mL, 2.5 mmol) was added dropwise at −78°C to a solution of chlorodiisopropylphosphine (175.5 mg, 1.15 mmol) in diethyl ether (5 mL). After warming to room temperature and removal of solvent, the product was extracted with dichloromethane. Volatile components were removed under vacuum and diisopropylphenylphosphine (134 mg, 61% yield) was obtained as colourless oil. Ph*Pi*Pr_2 (134 mg, 0.69 mmol) was added to an orange suspension of $[Rh(\mu\text{-}Cl)(CO)_2]_2$ (270 mg, 0.69 mmol) in dichloromethane (5 mL) at −40°C. The solution quickly turned yellow upon warming to room temperature. Subsequently the solvent was removed in vacuo and the residue was washed with pentane. [RhCl(CO)(*i*Pr_2PPh)$_2$] was isolated as a yellow solid from a saturated dichloromethane solution at −40°C (200 mg, 80%). IR ($CDCl_3$): $\tilde{\nu}$ = 1966.7 cm^{-1}; $^{31}P\{^1H\}$ NMR (121.5 MHz, $CDCl_3$, 25°C): δ = 44.6 ppm (d, ^1J(Rh,P) = 125 Hz).

[$PtCl_2$(dpb)] 7: A solution of $[PtCl_2(cod)]$ (150 mg, 0.40 mmol) in CH_2Cl_2 (5 mL) was added at −78°C to a solution of DPB **1** (200 mg, 0.42 mmol) in CH_2Cl_2 (5 mL). After warming to RT and subsequent stirring for 2 h, the volatiles were removed and the solid was extracted with THF. The supernatant was cooled at −40°C and complex **7** was collected by filtration. White crystals (169 mg, 57%) suitable for X-ray crystallography were obtained from a saturated THF solution at −40°C. M.p. 271–273°C; ^{31}P NMR (202.5 MHz, $CDCl_3$, 25°C): δ = 39.7 (dd, ^1J(Pt,P) = 3323.3 Hz, ^2J(P,P) = 9.0 Hz, P), 38.8 ppm (dd, ^1J(Pt,P) = 3081.3 Hz, ^2J(P,P) = 9.0 Hz, P); ^{11}B NMR (160.5 MHz, $CDCl_3$, 25°C): δ = 42.8 ppm; ^{195}Pt NMR (107.6 MHz, $CDCl_3$, 25°C): δ = −3957.4 ppm (^1J(Pt,P) = 3323.3 Hz, ^1J(Pt,P) = 3081.3 Hz); ^1H NMR (500.3 MHz, $CDCl_3$, 25°C): δ = 8.38 (d, ^3J(H,H) = 7.3 Hz, 1H; H_{arom}), 7.76 (dd, ^3J(H,H) = 8.0 Hz, ^3J(P,H) = 8.0 Hz, 1H; H_{arom}), 7.55 (dd, ^3J(H,H) = 7.8 Hz, ^3J(P,H) = 7.8 Hz, 1H; H_{arom}), 7.38 (pseudo-t, ^3J(H,H) = 6.8 Hz, 1H; H_{arom}), 7.33–7.20 (m, 6H; H_{arom}), 7.04 (m, 2H; H_{arom}), 6.86 (d, ^3J(H,H) = 6.7 Hz, 1H; H_{arom}), 3.86 (m, 1H; CH P*i*Pr_2), 3.12 (m, 1H; CH P*i*Pr_2), 2.74 (m, 1H; CH P*i*Pr_2), 1.84–1.80 (m, 6H; CH_3 P*i*Pr_2), 1.77 (dd, ^3J(P,H) = 5, ^3J(H,H) = 5 Hz, 3H; CH_3 P*i*Pr_2), 1.73 (dd, ^3J(P,H) = 5, ^3J(H,H) = 5 Hz, 3H; CH_3 P*i*Pr_2), 1.68 (m, 1H; CH P*i*Pr_2), 1.59 (dd, ^3J(P,H) = 15.9, ^3J(H,H) = 7.1 Hz, 3H; CH_3 P*i*Pr_2), 1.24 (dd, ^3J(P,H) = 14.4, ^3J(H,H) = 7.2 Hz, 3H; CH_3 P*i*Pr_2), 1.04 (dd, ^3J(P,H) = 16.7, ^3J(H,H) = 7.4 Hz, 3H; CH_3 P*i*Pr_2), 0.45 ppm (dd, ^3J(P,H) = 15.1 Hz, ^3J(H,H) = 7.3 Hz, 3H; CH_3 P*i*Pr_2); ^{13}C NMR (125.8 MHz, $CDCl_3$, 25°C): δ = 160.6 (d, ^2J(P,C) = 25.0 Hz; BC_{ipso} BPh), 160.0 (d, ^2J(P,C) = 25.3 Hz; BC_{ipso} BPh), 146.9 (s; C_{arom}), 141.8 (s; C_{arom}), 136.5 (d, ^1J(P,C) = 62.8 Hz; PC_{ipso}), 136.2 (s; C_{arom}), 133.8 (d, ^1J(P,C) = 56.2 Hz; PC_{ipso}), 131.8 (d, ^3J(P,C) = 18.9 Hz; C_{arom}), 131.7 (d, ^3J(P,C) = 18.4 Hz; C_{arom}), 130.6 (d, ^2J(P,C) = 4.0 Hz; C_{arom}), 130.3 (s; C_{arom}), 129.6 (s; 2 C_{arom}), 129.3 (d, ^2J(P,C) = 3.9 Hz; C_{arom}), 128.0 (s; C_{arom}), 126.5 (d, J(P,C) = 8.4 Hz; C_{arom}), 126.2 (d, J(P,C) = 7.5 Hz; C_{arom}), 125.6 (s; C_{arom}), 30.4 (d, ^1J(P,C) = 29.5 Hz; CH P*i*Pr_2), 29.1 (d, ^1J(P,C) = 32.7 Hz; CH P*i*Pr_2), 28.7 (d, ^1J(P,C) = 35.6 Hz; CH P*i*Pr_2), 24.5 (d, ^1J(P,C) = 23.6 Hz; CH P*i*Pr_2), 24.0 (s; CH_3 P*i*Pr_2), 23.8 (d, ^2J(P,C) = 3.2 Hz; CH_3 P*i*Pr_2), 22.1 (d, ^2J(P,C) = 3.1 Hz; CH_3 P*i*Pr_2), 21.9 (d, ^2J(P,C) = 5.2 Hz; CH_3 P*i*Pr_2), 20.9 (d, ^2J(P,C) = 7.8 Hz; CH_3 P*i*Pr_2), 20.8 (d, ^2J(P,C) = 10.4 Hz; CH_3 P*i*Pr_2), 20.7 (d, ^2J(P,C) = 2.0 Hz; CH_3 P*i*Pr_2), 18.7 ppm (s; CH_3 P*i*Pr_2).

[$PdCl_2$(dpb)] (8): A solution of $[PdCl_2(cod)]$ (90 mg, 0.32 mmol) in CH_2Cl_2 (5 mL) was added at −78°C to a solution of DPB **1** (150 mg, 0.32 mmol) in CH_2Cl_2 (5 mL). After warming to RT and subsequent stirring for 1 h, the volatile components were removed in vacuo and the resulting solid was extracted with toluene (5 mL). Yellow crystals suitable for X-ray crystallography (54 mg, 26%) were obtained by slow pentane diffusion into a dichloromethane solution at room temperature. M.p. 156–158°C; ^{31}P NMR (202.5 MHz, $CDCl_3$, 25°C): δ = 61.1 (d, ^2J(P,P) = 6.5 Hz, P), 56.0 ppm (d, ^2J(P,P) = 6.5 Hz, P); ^{11}B NMR (160.5 MHz, $CDCl_3$, 25°C): δ = 47.0 ppm; ^1H NMR (500.3 MHz, $CDCl_3$, 25C): δ = 8.49 (br, 1H; H_{arom}), 7.83 (dd, ^3J(H,H) = 6.7 Hz, ^3J(P,H) = 6.7 Hz, 1H; H_{arom}), 7.63 (dd, ^3J(H,H) = 8.3 Hz, ^3J(P,H) = 8.3 Hz, 1H; H_{arom}), 7.49 (br, 1H; H_{arom}), 7.45 (pseudo-t, ^3J(H,H) = 6.1 Hz, 1H; H_{arom}), 7.44 (pseudo-t, ^3J(H,H) = 6.3 Hz, 1H; H_{arom}), 7.39 (pseudo-t, ^3J(H,H) = 8.1 Hz, 1H; H_{arom}), 7.38 (pseudo-t, ^3J(H,H) = 10.3 Hz, 1H; H_{arom}), 7.34 (pseudo-t, ^3J(H,H) = 8.5 Hz, 1H; H_{arom}), 7.24 (d, ^3J(H,H) = 7.0 Hz, 1H; H_{arom}), 7.16 (br s, 1H; H_{arom}), 7.09 (d, ^3J(H,H) = 6.5 Hz, 1H; H_{arom}), 7.05 (br, 1H; H_{arom}), 3.98 (septd, ^2J(P,H) = 11.7, ^3J(H,H) = 5.9 Hz, 1H; CH P*i*Pr_2), 2.96 (septd, ^2J(P,H) = 11.2, ^3J(H,H) = 5.6 Hz, 1H; CH P*i*Pr_2), 2.69 (septd, ^2J(P,H) = 7.9, ^3J(H,H) = 3.9 Hz, 1H; CH P*i*Pr_2), 1.91 (dd, ^3J(P,H) = 18.8, ^3J(H,H) = 7.4 Hz, 3H; CH_3 P*i*Pr_2), 1.85 (dd, ^3J(P,H) = 19.0, ^3J(H,H) = 7.6 Hz, 3H; CH_3 P*i*Pr_2), 1.83 (dd, ^3J(P,H) = 19.8, ^3J(H,H) = 8.4 Hz, 3H; CH_3 P*i*Pr_2), 1.74 (dd, ^3J(P,H) = 12.8, ^3J(H,H) = 7.1 Hz, 3H; CH_3 P*i*Pr_2), 1.59 (dd, ^3J(P,H) = 15.8, ^3J(H,H) = 6.9 Hz, 3H; CH_3 P*i*Pr_2), 1.44 (m, 1H; CH P*i*Pr_2), 1.24 (dd, ^3J(P,H) = 14.1, ^3J(H,H) = 7.1 Hz, 3H; CH_3 P*i*Pr_2), 1.04 (dd, ^3J(P,H) = 16.4, ^3J(H,H) = 7.4 Hz, 3H; CH_3 P*i*Pr_2), 0.54 ppm (dd, ^3J(P,H) = 13.7, ^3J(H,H) = 7.5 Hz, 3H; CH_3 P*i*Pr_2); ^{13}C NMR (125.8 MHz, 25°C, $CDCl_3$): δ = 157.3 (d, ^2J(P,C) = 22.9 Hz; BC_{ipso}), 155.9 (d, ^2J(C,P) = 30.7 Hz; BC_{ipso}), 144.9 (s; BC_{ipso} BPh), 143.2 (s; C_{arom}), 138.3 (d, ^1J(P,C) = 52.8 Hz; PC_{ipso}), 137.8 (s; C_{arom}), 134.5 (d, ^1J(P,C) = 48.7 Hz; PC_{ipso}), 133.2 (d, ^3J(P,C) = 17.9 Hz; C_{arom}), 132.2 (s; C_{arom}), 131.5 (d, ^3J(P,C) = 17.3 Hz; C_{arom}), 131.3 (d, ^2J(P,C) = 4.0 Hz; C_{arom}), 130.2 (s; C_{arom}), 129.5 (s; C_{arom}), 129.2 (s; C_{arom}), 128.5 (br; C_{arom}), 127.7 (d, J(P,C) = 12.5 Hz; C_{arom}), 126.7 (d, J(P,C) = 10.2 Hz; C_{arom}), 125.8 (br; C_{arom}), 31.3 (d, ^1J(P,C) = 19.7 Hz; CH P*i*Pr_2), 31.1 (d, ^1J(P,C) = 25.3 Hz; CH P*i*Pr_2), 30.6 (d, ^1J(P,C) = 28.8 Hz; CH P*i*Pr_2), 25.5 (d, ^1J(P,C) = 16.6 Hz; CH P*i*Pr_2), 24.7 (br; CH_3 P*i*Pr_2), 24.6 (br; CH_3 P*i*Pr_2), 22.4 (br; CH_3 P*i*Pr_2), 21.7 (br; CH_3 P*i*Pr_2),

21.5 (br; CH_3 P*i*Pr$_2$), 21.3 (br; CH_3 P*i*Pr$_2$), 21.1 (s; CH_3 P*i*Pr$_2$), 18.7 ppm (s; CH_3 P*i*Pr$_2$); MS (DCI/NH_3): *m/z* (%): 670 (5) $[M+NH_4]^+$, 653 (6) $[M+H]^+$, 584 (100) $[M+NH_4-2i\text{Pr}]^+$, 531 (15) $[M-2i\text{Pr}-\text{Cl}]^+$.

Crystal structure determinations: Data were collected on a Bruker-AXS CCD 1000 diffractometer using an oil-coated shock-cooled crystal. Semi-empirical absorption corrections were employed.[36] The structure was solved by direct methods (SHELXS-97),[37] and refined using the least-squares method on F^2.[38]

Crystal data for 6a/6b: $C_{31}H_{41}BClOP_2Rh$, $M=640.75$, triclinic, space group $P\bar{1}$, $a=9.6067(6)$, $b=9.7896(6)$, $c=16.9491(11)$ Å, $\alpha=100.5110(10)$, $\beta=101.6460(10)$, $\gamma=98.5300(10)°$, $V=1506.34(16)$ Å^3, $Z=2$, $\rho_{calcd}=1.413$ g cm^{-3}, $F(000)=664$, $T=120(2)$ K, crystal size $0.2\times0.2\times0.1$ mm^3, 12 407 reflections collected (6528 independent, $R_{int}=0.0307$), $2\theta\leq54.0°$, 349 parameters, $R1$ $[I>2\sigma(I)]=0.0361$, $wR2$ [all data] = 0.0734, largest diff. peak and hole: 0.649 and −0.631 e Å^{-3}.

Crystal data for 7: $C_{38}H_{57}BCl_2OP_2Pt$, $M=884.58$, monoclinic, space group $P2_1/n$, $a=11.9425(14)$, $b=16.769(2)$, $c=19.876(2)$ Å, $\beta=106.3654(2)°$, $V=3819.2(8)$ Å^3, $Z=4$, $\rho_{calcd}=1.538$ g cm^{-3}, $F(000)=1792$, $T=133(2)$ K, crystal size $0.2\times0.2\times0.3$ mm^3, 21 825 reflections collected (7799 independent, $R_{int}=0.0257$), $2\theta\leq52.9°$, 423 parameters, $R1$ $[I>2\sigma(I)]=0.0250$, $wR2$ [all data] = 0.0647, largest diff. peak and hole: 1.037 and −2.335 e Å^{-3}.

Crystal data for 8: $C_{31}H_{43}BCl_4P_2Pd$, $M=736.6$, monoclinic, space group $C2/c$, $a=33.908(2)$, $b=10.0051(7)$, $c=20.1894(13)$ Å, $\beta=96.6600(10)°$, $V=6803.1(8)$ Å^3, $Z=8$, $\rho_{calcd}=1.438$ g cm^{-3}, $F(000)=3024$, $T=173(2)$ K, crystal size $0.1\times0.1\times0.2$ mm^3, 19 443 reflections collected (6961 independent, $R_{int}=0.0507$), $2\theta\leq52.8°$, 388 parameters, $R1$ $[I>2\sigma(I)]=0.0367$, $wR2$ [all data] = 0.0757, largest diff. peak and hole: 0.737 and −0.401 e Å^{-3}.

CCDC-652832–652834 contain the supplementary crystallographic data for this paper. These data can be obtained free of charge from The Cambridge Crystallographic Data Centre via www.ccdc.cam.ac.uk/data_request/cif.

Computational details: Calculations have been performed with the Gaussian 03 suite of programs,[39,40] at the DFT level of theory[41] using the hybrid functional B3PW91.[42] The basis set-RECP (relativistic effective core potential) SDD[43] was retained for Rh, Pt and Pd and the 6-31G** double-ζ basis set was used for all other atoms (C, P, B, Cl, N, O and H). The optimized structures were confirmed as true minima on the potential energy through vibrational analysis. The frequencies were calculated with analytical second derivatives. All total energies have been zero-point energy (ZPE) and temperature corrected using unscaled density functional frequencies. Natural Bond Orbital (NBO) analyses[44] were performed with the NBO-3.1 program to gain more insight into the M→B interactions. The corresponding Natural Localized Molecular Orbitals (NLMO) were plotted by using the molecular graphic package Molekel.[45] These calculations provided the following data: NBO stabilizing energy, percentage of the donor and acceptor NBO in the corresponding NLMO, occupancy of the donor and acceptor NBO orbitals, energy difference between the donor and acceptor NBO orbitals, off-diagonal NBO Fock matrix element, NPA atomic charge of boron and atom–atom net linear bond order based on the NLMO/NPA. Detailed computational results and cartesian coordinates for the optimized geometries of complexes **3***, **6a–c***, **7*** and **8*** at the B3PW91/SDD(M),6-31G**(other atoms) level of theory are included in the Supporting Information.

Acknowledgements

We are grateful to the CNRS, UPS, ANR program (project BILI) and Royal Society (International Joint Project Europe) for financial support of this work, and to IDRIS (CNRS, Orsay, France) for calculation facilities. Dr. Laurent Maron (LPCNO, Toulouse, France) and Professor Todd B. Marder (Durham, UK) are warmly acknowledged for helpful discussions. We also thank Dr. H. Gornitzka for his assistance in the X-ray diffraction analysis of complexes **7** and **8**.

[1] For general reviews dealing with transition-metal complexes of Group 13 elements, see: a) H. Wadepohl, *Angew. Chem.* **1997**, *109*, 2547–2550; *Angew. Chem. Int. Ed.* **1997**, *36*, 2441–2444; b) H. Braunschweig, *Angew. Chem.* **1998**, *110*, 1882–1898; *Angew. Chem. Int. Ed.* **1998**, *37*, 1786–1801; c) G. J. Irvine, M. J. Lesley, T. B. Marder, N. C. Norman, C. R. Rice, E. G. Robins, W. R. Roper, G. R. Whittell, L. J. Wright, *Chem. Rev.* **1998**, *98*, 2685–2722; d) R. A. Fischer, J. Weiß, *Angew. Chem.* **1999**, *111*, 3002–3022; *Angew. Chem. Int. Ed.* **1999**, *38*, 2830–2850; e) M. R. Smith III, *Prog. Inorg. Chem.* **1999**, *48*, 505–567; f) H. Braunschweig, M. Colling, *Coord. Chem. Rev.* **2001**, *223*, 1–51; g) N. N. Greenwood, *Coord. Chem. Rev.* **2002**, *226*, 61–69; h) H. Braunschweig, M. Colling, *Eur. J. Inorg. Chem.* **2003**, 393–403; i) S. Aldridge, D. L. Coombs, *Coord. Chem. Rev.* **2004**, *248*, 535–559; j) H. Braunschweig, C. Kollann, D. Rais, *Angew. Chem.* **2006**, *118*, 5380–5400; *Angew. Chem. Int. Ed.* **2006**, *45*, 5254–5274.

[2] a) J. M. Burlitch, M. E. Leonowicz, R. B. Petersen, R. E. Hughes, *Inorg. Chem.* **1979**, *18*, 1097–1105; b) H. Braunschweig, K. Gruss, K. Radacki, *Angew. Chem.* **2007**, *119*, 7929–7931; *Angew. Chem. Int. Ed.* **2007**, *46*, 7782–7784.

[3] J. T. Golden, T. H. Peterson, P. L. Holland, R. G. Bergman, R. A. Andersen, *J. Am. Chem. Soc.* **1998**, *120*, 223–224.

[4] The borane analogue of complex **A** has only been spectroscopically characterized: J. M. Burlitch, J. H. Burk, M. E. Leonowicz, R. E. Hughes, *Inorg. Chem.* **1979**, *18*, 1702–1709.

[5] Early claims for transition metal–borane complexes a) D. F. Shriver, *J. Am. Chem. Soc.* **1963**, *85*, 3509–3510; b) G. W. Parshall, *J. Am. Chem. Soc.* **1964**, *86*, 361–364; c) M. P. Johnson, D. F. Shriver, *J. Am. Chem. Soc.* **1966**, *88*, 301–304 were not supported by structural authentication and their real identity has been strongly questioned by Braunschweig et al. d) H. Braunschweig, T. Wagner, *Chem. Ber.* **1994**, *127*, 1613–1614; e) H. Braunschweig, T. Wagner, *Z. Naturforsch. B* **1996**, *51*, 1618–1620; f) H. Braunschweig, C. Kollann, *Z. Naturforsch. B* **1999**, *54*, 839–842.

[6] A. F. Hill, G. R. Owen, A. J. P. White, D. J. Williams, *Angew. Chem.* **1999**, *111*, 2920–2923; *Angew. Chem. Int. Ed.* **1999**, *38*, 2759–2761.

[7] a) M. R. St.-J. Foreman, A. F. Hill, A. J. P. White, D. J. Williams, *Organometallics* **2004**, *23*, 913–916; b) I. R. Crossley, A. F. Hill, *Organometallics* **2004**, *23*, 5656–5658; c) D. J. Mihalcik, J. L. White, J. M. Tanski, L. N. Zakharov, G. P. A. Yap, C. D. Incarvito, A. L. Rheingold, D. Rabinovitch, *Dalton Trans.* **2004**, 1626–1634; d) I. R. Crossley, M. R. St.-J. Foreman, A. F. Hill, A. J. P. White, D. J. Williams, *Chem. Commun.* **2005**, 221–223; e) I. R. Crossley, A. F. Hill, E. R. Humphrey, A. C. Willis, *Organometallics* **2005**, *24*, 4083–4086; f) I. R. Crossley, A. F. Hill, A. C. Willis, *Organometallics* **2006**, *25*, 289–299; g) V. K. Landry, J. G. Melnick, D. Buccella, K. Pang, J. C. Ulichny, G. Parkin, *Inorg. Chem.* **2006**, *45*, 2588–2597; h) R. J. Blagg, J. P. H. Charmant, N. G. Connelly, M. F. Haddow, A. G. Orpen, *Chem. Commun.* **2006**, 2350–2352; i) J. S. Figueroa, J. G. Melnick, G. Parkin, *Inorg. Chem.* **2006**, *45*, 7056–7058; j) K. Pang, S. M. Quan, G. Parkin, *Chem. Commun.* **2006**, 5015–5017; k) I. R. Crossley, A. F. Hill, A. C. Willis, *Organometallics* **2005**, *24*, 1062–1064.

[8] Metal→boron interactions have also been proposed to account for the bent structure of metallocenylboranes, and the delocalized through-space nature of such M→B interactions has been recently established theoretically for ferrocenylboranes: see a) M. Scheibitz, M. Bolte, J. W. Bats, H.-W. Lerner, I. Nowik, R. H. Herber, A. Krapp, M. Lein, M. C. Holthausen, M. Wagner, *Chem. Eur. J.* **2005**, *11*, 584–603; b) K. Venkatasubbaiah, L. N. Zakharov, W. S. Kassel, A. L. Rheingold, F. Jäkle, *Angew. Chem.* **2005**, *117*, 5564–5569; *Angew. Chem. Int. Ed.* **2005**, *44*, 5428–5433 and references therein.

[9] Spectroscopic evidence for Ta→B interactions has been reported for BH_3 and $PhBCl_2$ adducts of $[Ta(OSi\textit{t}Bu_3)_3]$: J. B. Bonanno, T. P. Henry, P. T. Wolczanski, A. W. Pierpont, T. R. Cundari, *Inorg. Chem.* **2007**, *46*, 1222–1232.

[10] For recent examples of M→B interactions within borylene complexes and metalloborylenes, see: a) H. Braunschweig, D. Rais, K.

Uttinger, *Angew. Chem.* **2005**, *117*, 3829–3832; *Angew. Chem. Int. Ed.* **2005**, *44*, 3763–3766; b) H. Braunschweig, K. Radacki, D. Rais, F. Seeler, *Angew. Chem.* **2006**, *118*, 1087–1090; *Angew. Chem. Int. Ed.* **2006**, *45*, 1066–1069; c) H. Braunschweig, C. Burschka, M. Burzler, S. Metz, K. Radacki, *Angew. Chem.* **2006**, *118*, 4458–4461; *Angew. Chem. Int. Ed.* **2006**, *45*, 4352–4355.

[11] The contribution of M→B interactions has also been pointed out in the bonding description of tantalocene–borataalkene η^2-complexes a) K. S. Cook, W. E. Piers, R. McDonald, *J. Am. Chem. Soc.* **2002**, *124*, 5411–5418 and references therein and of boryl-bridged complexes b) D. Curtis, M. J. G. Lesley, N. C. Norman, A. G. Orpen, J. Starbuck, *J. Chem. Soc. Dalton Trans.* **1999**, 1687–1694; c) S. A. Westcott, T. B. Marder, R. T. Baker, R. L. Harlow, J. C. Calabrese, K. C. Lam, Z. Lin, *Polyhedron* **2004**, *23*, 2665–2677; d) H. Braunschweig, K. Radacki, D. Rais, G. R. Whittell, *Angew. Chem.* **2005**, *117*, 1217–1219; *Angew. Chem. Int. Ed.* **2005**, *44*, 1192–1193.

[12] For the synthesis, structure and coordination properties of PB and PBP systems, see: a) S. Bontemps, H. Gornitzka, G. Bouhadir, K. Miqueu, D. Bourissou, *Angew. Chem.* **2006**, *118*, 1641–1644; *Angew. Chem. Int. Ed.* **2006**, *45*, 1611–1614; b) S. Bontemps, G. Bouhadir, K. Miqueu, D. Bourissou, *J. Am. Chem. Soc.* **2006**, *128*, 12056–12057; c) S. Bontemps, G. Bouhadir, P. W. Dyer, K. Miqueu, D. Bourissou, *Inorg. Chem.* **2007**, *46*, 5149–5151; d) M. W. P. Bebbington, G. Bouhadir, D. Bourissou, *Eur. J. Org. Chem.* **2007**, 4483–4486; e) M. Sircoglou, S. Bontemps, M. Mercy, N. Saffon, M. Takahashi, G. Bouhadir, L. Maron, D. Bourissou, *Angew. Chem.* DOI: 10.1002/ange.20073518; *Angew. Chem. Int. Ed.* DOI: 10.1002/anie.200703518. For the synthesis, structure and coordination properties of a related NB system, see f) J. Vergnaud, T. Ayed, K. Hussein, L. Vendier, M. Grellier, G. Bouhadir, J.-C. Barthelat, S. Sabo-Etienne, D. Bourissou, *Dalton Trans.* **2007**, 2370–2372.

[13] A few transition-metal complexes of PBP systems with borane moieties free of interaction with any basic site have also been reported: a) L. Turculet, J. D. Feldman, T. D. Tilley, *Organometallics* **2004**, *23*, 2488–2502; b) J. C. Thomas, J. C. Peters, *Polyhedron* **2004**, *23*, 2901–2913.

[14] For the derivatization of PB compounds into photoisomerizable systems, see: M. W. P. Bebbington, S. Bontemps, G. Bouhadir, D. Bourissou, *Angew. Chem.* **2007**, *119*, 3397–3400; *Angew. Chem. Int. Ed.* **2007**, *46*, 3333–3336.

[15] For transition-metal complexes deriving from a PSB ligand, see: a) D. J. H. Emslie, J. M. Blackwell, J. F. Britten, L. E. Harrington, *Organometallics* **2006**, *25*, 2412–2414; b) S. R. Oakley, K. D. Parker, D. J. H. Emslie, I. Vargas-Baca, C. M. Robertson, L. E. Harrington, J. F. Britten, *Organometallics* **2006**, *25*, 5835–5838.

[16] Intramolecular activation of an Ni–CH_3 bond was proposed to be responsible for the spectacular rate enhancement observed in $PhSiH_3$ dehydrogenative oligomerization in the presence of an ambiphilic PAl system: F.-G. Fontaine, D. Zargarian, *J. Am. Chem. Soc.* **2004**, *126*, 8786–8794.

[17] Anchoring substrates by interaction with pendant Lewis acid moieties has been investigated with boron analogues of the DIOP ligand: a) A. Börner, J. Ward, K. Kortus, H. B. Kagan, *Tetrahedron: Asymmetry* **1993**, *4*, 2219–2228; b) L. B. Fields, E. N. Jacobsen, *Tetrahedron: Asymmetry* **1993**, *4*, 2229–2240.

[18] The solid-state structure of the related {RhCl(CO)[$Me_2PC(Me)$=$C(Me)BMe_2]_2$} complex reported by Grobe et al. revealed large Rh–B distances of (2.94–2.97 Å) and an almost planar environment around the boron atoms, suggesting a very weak, if any, Rh→B interaction: a) J. Grobe, R. Martin, *Z. Anorg. Chem.* **1992**, *607*, 146–152; b) J. Grobe, K. Lütz-Brotchrup, B. Krebs, M. Läge, H.-H. Niemeyer, E.-U. Würthwein, *Z. Naturforsch.* **2006**, *61b*, 882–895.

[19] C. A. Tolman, *Chem. Rev.* **1977**, *77*, 313–348.

[20] For general reviews, see for example a) D. Bourissou, O. Guerret, F. P. Gabbaï, G. Bertrand, *Chem. Rev.* **2000**, *100*, 39–91; b) W. A. Herrmann, *Angew. Chem.* **2002**, *114*, 1342–1363; *Angew. Chem. Int. Ed.* **2002**, *41*, 1290–1309.

[21] For selected recent examples, see: a) V. Lavallo, J. Mafhouz, Y. Canac, B. Donnadieu, W. W. Schoeller, G. Bertrand, *J. Am. Chem. Soc.* **2004**, *126*, 8670–8671; b) D. Martin, A. Baceiredo, H. Gornitzka, W. W. Schoeller, G. Bertrand, *Angew. Chem.* **2005**, *117*, 1728–1731; *Angew. Chem. Int. Ed.* **2005**, *44*, 1700–1703; c) V. Lavallo, Y. Canac, C. Prasang, B. Donnadieu, G. Bertrand, *Angew. Chem.* **2005**, *117*, 5851–5855; *Angew. Chem. Int. Ed.* **2005**, *44*, 5705–5709; d) M. Alcarazo, S. J. Roseblade, A. R. Cowley, R. Fernández, J. M. Brown, J. M. Lassaletta, *J. Am. Chem. Soc.* **2005**, *127*, 3290–3291; e) Y. Canac, S. Conejero, B. Donnadieu, W. W. Schoeller, G. Bertrand, *J. Am. Chem. Soc.* **2005**, *127*, 7312–7313; f) C. Präsang, B. Donnadieu, G. Bertrand, *J. Am. Chem. Soc.* **2005**, *127*, 10182–10183; g) M. D. Sanderson, J. W. Kamplain, C. W. Bielawski, *J. Am. Chem. Soc.* **2006**, *128*, 16514–16515; h) E. Mas-Marzá, J. A. Mata, E. Peris, *Angew. Chem.* **2007**, *119*, 3803–3805; *Angew. Chem. Int. Ed.* **2007**, *46*, 3729–3731; i) S. Gómez-Bujedo, M. Alcarazo, C. Pichon, E. Álvarez, R. Fernández, J. M. Lassaletta, *Chem. Commun.* **2007**, 1180–1182; j) P. Bazinet, T.-G. Ong, J. S. O'Brien, N. Lavoie, E. Bell, G. P. A. Yap, I. Korobkov, D. S. Richeson, *Organometallics* **2007**, *26*, 2885–2895.

[22] A Cambridge Structural Database (F. H. Allen, *Acta Crystallogr.* **2002**, *B58*, 380–388) search revealed only a few structurally authenticated *cis*-[Rh(CO)Cl(diphos)] complexes: a) K. A. Bunten, D. H. Farrar, A. J. Poë, A. Lough, *Organometallics* **2002**, *21*, 3344–3350; b) S. A. Laneman, F. R. Fronczek, G. G. Staneley, *J. Am. Chem. Soc.* **1988**, *110*, 5585–5586; c) A. Suarez, M. A. Mendez-Rojas, A. Pizzano, *Organometallics* **2002**, *21*, 4611–4621; d) R. Paciello, L. Siggel, H. J. Kneuper, N. Walker, M. Roper, *J. Mol. Catal. A: Chem.* **1999**, *143*, 85–97.

[23] The change from *cis* to *trans* coordination is accompanied by a widening of both the PCC and CCB bond angles by about 4°.

[24] This situation is reminiscent to that observed with related diphosphines featuring a diphenyl ether tether: a) P. Dierkes, P. W. N. M. van Leeuwen, *J. Chem. Soc. Dalton Trans.* **1999**, 1519–1529; b) Z. Freixa, P. W. N. M. van Leeuwen, *Dalton Trans.* **2003**, 1890–1901.

[25] The short distance between the carbon atom of the CO group and the *ipso*-carbon of the phenyl ring at boron (3.107 Å) in compound **6a** may suggest some π···π interaction. For a recent example of such contacts between carbonyl ligands and an aryl ring, see D. L. Reger, R. P. Watson, M. D. Smith, P. J. Pellechia, *Organometallics* **2005**, *24*, 1544–1555.

[26] The optimized geometry of **6a*** reproduces the short distance (3.118 Å) observed experimentally (3.107 Å) between the carbon atom of the CO group and the *ipso*-carbon of the phenyl ring at boron. In a similar way, the *cis* isomer **6c*** is predicted to also feature such a short CC distance (3.026 Å).

[27] DFT calculations predict very similar $\tilde{\nu}$(CO) values for both complexes **6a*** (2076 cm^{-1}) and **6b*** (2075 cm^{-1}), but a significantly higher value for the related *cis* complex **6c*** (2125 cm^{-1}).

[28] *trans*-[$RhCl(CO)L_2$] complexes featuring phosphonite and phosphite ligands typically exhibit $\tilde{\nu}$(CO) values ranging from 1990 to 2020 cm^{-1}: see a) J. I. Van der Vlugt, R. Sablong, P. C. M. M. Magusin, A. M. Mills, A. L. Spek, D. Vogt, *Organometallics* **2004**, *23*, 3177–3183; b) E. Fernandez, A. Ruiz, C. Claver, S. Castillon, *Organometallics* **1998**, *17*, 2857–2864.

[29] The ^1J(Rh,P) coupling constant for both [RhCl(CO)(dpb)] complexes **6a** and **6b** (102 Hz) is significantly lower than that measured for the borane-free complex *trans*-[$RhCl(CO)(i Pr_2PPh)_2$] (126 Hz). This difference may also be attributed to the reduced electron density at rhodium.

[30] a) High carbonyl stretching frequencies have already been noticed for some metallaboratranes[6,7a,h,i,10] and a heterodinuclear complex of an ambiphilic PSB ligand;[15b] but comparison with related complexes without σ-acceptor ligand was not readily possible.

[31] Unsymmetrical *trans*-[$PdCl_2$(diphosphine)] complexes typically exhibit ^2J(P,P) coupling constants greater than 500 Hz. See for example: O. Grossman, C. Azerraf, D. Gelman, *Organometallics* **2006**, *25*, 375–381.

[32] *trans*-[$PtCl_2$(diphosphine)] complexes typically exhibit ^1J(Pt,P) coupling constants of around 2500 Hz: C. A. Bessel, P. Aggarwal, A. C. Marschilok, K. J. Takeuchi, *Chem. Rev.* **2001**, *101*, 1031–1066.

[33] P. Braunstein, U. Englert, G. E. Herberich, M. Neuschütz, *Angew. Chem.* **1995**, *107*, 1090–1092; *Angew. Chem. Int. Ed.* **1995**, *34*, 1010–1012.
[34] a) D. F. Shriver, *Acc. Chem. Res.* **1970**, *3*, 231–238; b) R. G. Pearson, *Chem. Rev.* **1985**, *85*, 41–49; c) R. J. Angelici, *Acc. Chem. Res.* **1995**, *28*, 51–60.
[35] a) A. F. Hill, *Organometallics* **2006**, *25*, 4741–4143; b) G. Parkin, *Organometallics* **2006**, *25*, 4744–4747.
[36] SADABS, Program for data correction, Bruker-AXS.
[37] G. M. Sheldrick, *Acta Crystallogr.* **1990**, *A46*, 467–473.
[38] SHELXL-97, Program for Crystal Structure Refinement, G. M. Sheldrick, University of Göttingen, **1997**.
[39] Gaussian 03, Revision B.05, M. J. Frisch, G. W. Trucks, H. B. Schlegel, G. E. Scuseria, M. A. Robb, J. R. Cheeseman, J. A. Montgomery, Jr. T. Vreven, K. N. Kudin, J. C. Burant, J. M. Millam, S. S. Iyengar, J. Tomasi, V. Barone, B. Mennucci, M. Cossi, G. Scalmani, N. Rega, G. A. Petersson, H. Nakatsuji, M. Hada, M. Ehara, K. Toyota, R. Fukuda, J. Hasegawa, M. Ishida, T. Nakajima, Y. Honda, O. Kitao, H. Nakai, M. X. Klene, Li, J. E. Knox, H. P. Hratchian, J. B. Cross, C. Adamo, J. Jaramillo, R. Gomperts, R. E. Stratmann, O. Yazyev, A. J. Austin, R. Cammi, C. Pomelli, J. W. Ochterski, P. Y. Ayala, K. Morokuma, G. A. Voth, P. Salvador, J. J. Dannenberg, V. G. Zakrzewski, S. Dapprich, A. D. Daniels, M. C. Strain, O. Farkas, D. K. Malick, A. D. Rabuck, K. Raghavachari, J. B. Foresman, J. V. Ortiz, Q. Cui, A. G. Baboul, S. Clifford, J. Cioslowski, B. B. Stefanov, G. Liu, A. Liashenko, P. Piskorz, I. Komaromi, R. L. Martin, D. J. Fox, T. Keith, M. A. Al-Laham, C. Y. Peng, A. Nanayakkara, M. Challacombe, P. M. W. Gill, B. Johnson, W. Chen, M. W. Wong, C. Gonzalez, J. A. Pople, Gaussian, Inc., Pittsburgh PA, **2003**.
[40] W. J. Hehre, L. Radom, P. v. R. Schleyer, J. A. Pople, *Ab Initio Molecular Orbital Theory*, Wiley, New York, **1986**.
[41] R. G. Parr, W. Yang, *Functional Theory of Atoms and Molecules* (Eds.: R. Breslow, J. B. Goodenough), Oxford University, New York, **1989**.
[42] a) A. D. Becke, *J. Chem. Phys.* **1993**, *98*, 5648–5652; b) K. Burke, J. P. Perdew, W. Yang, *Electronic Density Functional Theory: Recent Progress and New Directions* (Eds.: J. F. Dobson, G. Vignale, M. P. Das), Plenum Press, New York, **1998**.
[43] a) M. Dolg, *Modern Methods and Algorithm of Quantum Chemistry, Vol. 1* (Ed.: J. Grotendorst), John von Neuman Institute for Computing, Jülich (Germany), **2000**, pp. 479–508; b) M. Dolg, U. Wedig, H. Stoll, H. Preuss, *J. Chem. Phys.* **1987**, *86*, 866–872; c) D. Andrae, U. Häussermann, M. Dolg, H. Stoll, H. Preuss, *Theor. Chim. Acta.* **1990**, *77*, 123–141.
[44] a) A. E. Reed, L. A. Curtiss, F. Weinhold, *Chem. Rev.* **1988**, *88*, 899–926; b) J. P. Foster, F. Weinhold, *J. Am. Chem. Soc.* **1980**, *102*, 7211–7218 .
[45] a) Molekel 4.3, P. Flükiger, H. P. Lüthi, S. Portmann, J. Weber, Swiss Center for Scientific Computing, Manno, Switzerland, 2000–2002; b) S. Portmann, H. P. Lüthi, *Chimica* **2000**, *54*, 766–770.

Received: July 4, 2007
Published online: October 19, 2007

